due solely to coordination of NO to **2**. The IR absorption at 1890 cm^{-1} denotes linear coordination of the nitrosyl ligand to the rhodium metal center.[21] According to the initial EXAFS analysis,[20] coordination of NO to **2** would result in a six-coordinate $\{MNO\}^8$ complex which would require the nitrosyl ligand to adopt a bent configuration.[23] Therefore, if **2** is the source of the nitrosyl species, either loss of the oxygen adduct ligand or a reversible change in surface coordination must occur. At this time, there is no evidence to rule out either effect.

4. Summary

Reaction of the μ-oxo carbonyl complex **1** with 30 Torr of NO at 100 °C resulted in the formation of the rhodium oxygen adduct **2** (80%) and rhodium nitrate/nitrite complex (20%) and was characterized by IR analysis and XPS. Comparison of the Rh $3d_{5/2}$ binding energies of **2** prepared via reaction of **1** and O_2 (310.1 eV) and of the NO-treated sample (310.1 eV) demonstrated the two to be identical within experimental error. XPS corroborated both the lack of nitrosyl coordination seen in IR and the sample's similarity to **2** in its reactivity for CO. The rhodium nitrate/nitrite complex was identified by IR (ν_{NO} = 1540 cm^{-1}), and an alternate assignment of this species to a carbonate complex was refuted by a ^{13}CO labeling experiment. No other nitrogen-containing products, either coordinated to the rhodium metal center or in the gas phase (e.g., N_2O), were observed by IR analysis. However, IR did detect CO_2 formation, which suggests that N_2 may be the primary nitrogen-containing product in this reaction.

Reaction of **1** with 70 Torr of NO at 400 °C was monitored by IR analysis. Both the decomposition of the rhodium nitrate/nitrite complex and the appearance of a nitrosyl species were observed. The nitrosyl species possessed a linearly coordinated NO ligand (ν_{NO} = 1890 cm^{-1}). Upon cooling and evacuation, the intensity of this absorption significantly decreased.

After the carbonyl complex **1** had been reacted with 30 Torr of NO at 100 °C, generating **2** and the nitrate/nitrite complex, **1** was regenerated from **2** by reaction with 30 Torr of CO at 100 °C. The rhodium nitrate/nitrite complex was unreactive toward CO under these conditions. More significantly, even after **1** had been reacted with 70 Torr of NO at 400 °C and formation of the nitrosyl species was observed, **1** was identified by IR as the primary product after treatment of the sample with 30 Torr of CO at 100 °C. In contrast to several of the previous investigations, only trace amounts of rhodium isocyanate, accounting for less than 2% of the total rhodium in the sample, was identified by IR analysis (ν_{NCO} = 2204 cm^{-1}). Formation of the isocyanate complex has been traced to the presence of rhodium aggregates; in separate experiments, conversion of dimeric complex **2** to a larger rhodium aggregate by treatment with H_2 resulted in a much greater yield of the isocyanate complex (27%) under milder reaction conditions.[24] In addition to decreasing the amount of active rhodium in the sample, isocyanate complex formation is undesirable since exposure to water will produce ammonia, which is tightly held and poisons the complex.[25] The ability to regenerate **1** demonstrates the integrity of the silica bonding and coordination to the rhodium metal center under the aforementioned reaction conditions. The catalytic behavior of these silica-attached rhodium complexes toward NO reduction by CO merits investigation.

Acknowledgment. This work was supported by the U.S. Department of Energy, Office of Basic Energy Sciences. We thank Jeff Cook for assistance with the XPS experiments.

(23) Enemark, J. H.; Feltham, R. D. *Coord. Chem. Rev.* **1974**, *13*, 339.

(24) Cannon, K. C.; White, J. M., manuscript in preparation.

(25) Unland, M. T. *J. Catal.* **1973**, *31*, 459.

Carbon K-Shell Excitation of Metallocenes

E. Rühl[†] and A. P. Hitchcock*

Contribution from the Department of Chemistry, McMaster University, Hamilton, Ontario, Canada L8S 4M1. *Received December 19, 1988*

Abstract: The C 1s oscillator strength spectra of $M(C_5H_5)_2$, M = Fe, Co, and Ni, have been derived from inelastic electron scattering spectra under conditions dominated by electric dipole transitions. The region below the C 1s ionization potential in each spectrum is dominated by two peaks which are assigned to C 1s $\rightarrow 4e_{1g}(d_{xz},d_{yz})$ and C 1s $\rightarrow 3e_{2u}(\pi^*)$ excitations. These spectra are dramatically different from that expected for the C 1s spectrum of the free cyclopentadienyl radical or the cyclopentadienyl anion, either of which should be dominated by a single, low-lying 1s $\rightarrow \pi^*$ transition. The intensity of the lower energy C 1s $\rightarrow 4e_{1g}$ transition is strongly dependent on the metal atom because of changes in the ground-state electron configurations. The results of extended Hückel theory calculations of the ground and C 1s excited states are found to be in qualitative agreement with the experimental results. The metallocene spectra are the first unambiguous experimental evidence for strong modification by metal bonding of the core excitation spectrum of a ligand. The spectra show that site-selective inner-shell excitation is a highly sensitive probe of the character of the unoccupied and partially filled molecular orbitals of organometallic compounds.

1. Introduction

Considerable attention is now being given to the electronic spectroscopy of organometallic compounds on account of their interesting and varied electronic structures and because they are useful models for the bonding of organic compounds to metal surfaces. Since the metallocene ("sandwich") compounds were discovered in 1951,[1] their electronic structure has been extensively studied by calculation[2] and by most standard spectroscopies. Spectroscopic studies of the unoccupied levels include electron transmission spectroscopy (ETS)[3,4] and valence excitation in the

[†] Permanent address: Institut für Physikalische Chemie, Freie Universität Berlin, Takustrasse 3, D-1000 Berlin 33, Federal Republic of Germany. Present address: Department of Chemistry, University of Colorado, Boulder, CO 80309.

(1) Kealy, T. J.; Pauson, P. L. *Nature* **1951**, *168*, 1039.

(2) Rohmer, M. M.; Veillard, V. *Chem. Phys.* **1975**, *11*, 349. Almoef, J.; Faegri, K.; Schilling, B. E. R.; Luethi, H. P. *Chem. Phys. Lett.* **1984**, *106*, 266. Hoejer, G.; Meeze-Hoejer, S.; Costas, M.; Martinez, J. *Chem. Phys.* **1978**, *27*, 381. Clark, D. W.; Warren, K. D. *Inorg. Chim. Acta* **1978**, *30*, 251.

(3) Modelli, A.; Foffani, A.; Guerra, M.; Jones, D.; Distefano, G. *Chem. Phys. Lett.* **1983**, *99*, 58.

0002-7863/89/1511-5069$01.50/0

visible and near ultraviolet.[5-8] In addition, the Fe K-shell X-ray absorption spectrum of gaseous ferrocene[9] and the metal K-shell spectra of solid ferrocene and nickelocene have been recorded and analyzed with the aid of multiple scattering calculations.[10]

Inner-shell excitation spectroscopy offers a useful complement to ETS and valence electron excitation as a means of investigating the unoccupied molecular orbitals of organometallic compounds. Inner-shell excitation measures a site-selected, dipole, partial density of states since the core hole localizes the excitation on a single atom. Thus C1s excitation energies and particularly transition intensities, which are primarily sensitive to the C_{2p} contributions to the optical orbital at the core-excited atom, can be a useful probe of the virtual orbitals of organic and organometallic molecules. As an example, the intensities of C 1s $\rightarrow \pi^*$ transitions have been used to study the effect of various substituents on the spatial distribution of the carbonyl π^* orbital in HCOX, X = F, OH, NH_2.[11] For the metallocences studied in this work C 1s $\rightarrow \pi^*$ intensities are used to probe the involvement of $C2p_z$ orbitals in the metal-ring bonding and antibonding orbitals.

Recently inner-shell electron energy loss spectroscopy (ISEELS) has been used to investigate several transition-metal carbonyls.[12-14] When the C 1s and O 1s spectra of the metal carbonyls are compared to those of free CO, the energies of the 1s $\rightarrow \pi^*$ and 1s $\rightarrow \sigma^*$ transitions are found to be very similar. The only remarkable change from the spectrum of free CO is that the oscillator strength of the C 1s $\rightarrow \pi^*$ transition [f(C 1s,π^*)] is somewhat reduced, and there is a systematic decline of f(C 1s,π^*) with increased d-electron count on the metal. The decrease in f(C 1s,π^*) has been interpreted as a measure of the extent of increased backbonding since the trends in the ISEELS results are consistent with other experimental determinations (e.g., IR, XPS) of the strength of backbonding in the compounds studied.[12]

In this paper we focus our interest on the cyclopentadienyl (Cp) aromatic ligand, π-complexed to transition metals. In sharp contrast to the metal carbonyls, where the shape of the spectra are largely independent of the metal atom, the metallocene C 1s spectra are very different from that expected for free Cp and are found to vary considerably with metal atom replacement. Extended Hückel calculations of the metallocenes are used to assist spectral assignment through the trends in virtual orbital energies and wave functions with metal type. The relationship of the energies of continuum C 1s $\rightarrow \sigma^*$(C–C) features and the C–C bond length is also discussed. Finally, the metallocene spectra are compared to the C 1s NEXAFS of a surface which is believed to consist of a monolayer of cyclopentadienyl (C_5H_5, Cp) on Pt(111).[15] This comparison demonstrates the utility of core excitation spectra of organometallics as models for NEXAFS studies of π-bonded chemisorbates on metal surfaces.

2. Experimental Section

The inner-shell electron energy loss spectrometer and operating techniques have been described previously.[16] Briefly, we measure the distribution of energy losses of an electron beam with a kinetic energy chosen so that the beam energy after inelastic collision is 2.5 keV. With this impact energy and an average scattering angle of 2°, primarily electric-dipole electronic transitions are excited. The resolution, limited mainly by the energy spread of the unmonochromated incident electron beam, was 0.7 eV FWHM. The metallocene samples were used as supplied from Strem Chemicals. The low vapor pressure of the solid compounds required the use of a direct inlet system with placement of the sample as close as possible to the scattering region.

The C1s spectra were converted to absolute optical oscillator strengths (f values) by using a conversion procedure described and tested previously.[17] The reproducibility of f values derived from independently recorded spectra is about 5%, whereas the absolute accuracy is about 20% according to comparisons with known optical oscillator strength data.[17]

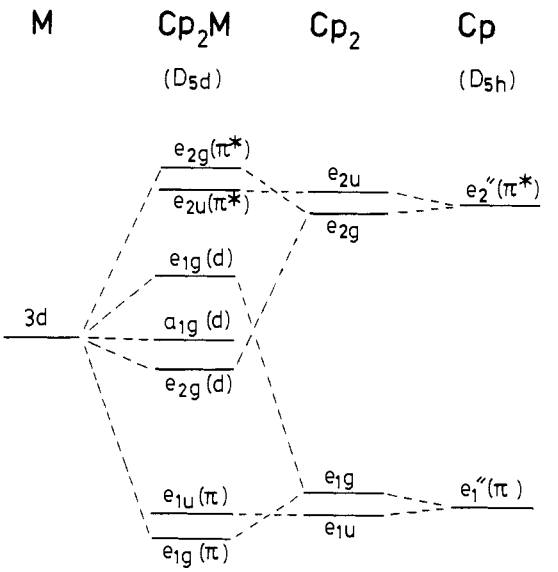

Figure 1. Qualitative molecular orbital diagram for the group 8b metallocenes.

3. Results and Discussion

3.1. Molecular Orbital Descriptions and Details of Extended Hückel Calculation. The frontier orbital electronic structure (D_{5d}) of the group 8b 3d-metallocenes is generally accepted to be[4,5]

$$Fe(Cp)_2: \quad (3e_{2g})^4(5a_{1g})^2(4e_{1g})^0(3e_{2u})^0(4e_{2g})^0$$

$$Co(Cp)_2: \quad (3e_{2g})^4(5a_{1g})^2(4e_{1g})^1(3e_{2u})^0(4e_{2g})^0$$

$$Ni(Cp)_2: \quad (3e_{2g})^4(5a_{1g})^2(4e_{1g})^2(3e_{2u})^0(4e_{2g})^0$$

A schematic indicating the metal (M) and cyclopentadienyl (Cp) origins of the molecular orbitals of metallocenes is presented in Figure 1. The molecular structure and bonding of the 3d metallocenes has been reviewed by Haaland.[18] In the gas-phase equilibrium conformation the Cp rings are eclipsed (D_{5h}). However, we use D_{5d} symmetry labels throughout this paper since this is the more commonly employed nomenclature owing to the belief from early X-ray crystallography that the staggered (D_{5d}) conformation was more stable.

We have used extended Hückel theory (EHT) calculations to aid our spectral interpretation. The experimental gas-phase, D_{5h} molecular geometries were employed in the calculation.[18] The metal-ring plane distances are 1.674, 1.741, and 1.834 Å for the Fe, Co, and Ni metallocenes.[18] The calculations were also carried out with the staggered, D_{5d} geometry of ferrocene and simple exchange of the metal atom. These latter results were found to be very similar to those obtained by using the correct experimental geometry, consistent with the known low barrier to rotation of π-bonded Cp rings. Two different sets of Hückel parameters, those given by Albright et al.[19] and those of Halet et al.,[20] were found to give identical orbital orderings and similar energies. The reported results are those derived by using the Hückel parameters

(4) Giordan, J. C.; Morre, J. H.; Tossell, J. A.; Weber, J. *J. Am. Chem. Soc.* **1983**, *105*, 3431. Giordan, J. C.; Morre, J. H.; Tossell, J. A. *Acc. Chem. Res.* **1986**, *19*, 281.
(5) Sohn, Y. S.; Hendrickson, D. N.; Gray, H. B. *J. Am. Chem. Soc.* **1971**, *93*, 3603. Switzer, M. E.; Wang, R.; Rettig, M. F.; Makai, A. H. *J. Am. Chem. Soc.* **1974**, *96*, 7669.
(6) Koch, E. E.; Otto, A. *Chem. Phys. Lett.* **1970**, *6*, 15. Gordon, K. R.; Warren, K. D. *Inorg. Chem.* **1978**, *17*, 987. Barton, T. J.; Grinter, R.; Thomson, A. J. *J. Chem. Soc., Dalton Trans.* **1979**, 1912.
(7) Weber, J.; Goursol, A.; Penigault, E.; Ammeter, J. H.; Bachman, J. *J. Am. Chem. Soc.* **1982**, *104*, 1491. Richer, G.; Sandorfy, C. *J. Mol. Struct. (Theochem)* **1985**, *123*, 74.
(8) Dowben, P. A.; Driscoll, D. C.; Tate, R. S.; Boag, N. M. *Organometallics* **1988**, *7*, 305.
(9) Joos, G.; Peter, K. H. *Z. Phys. Chem. NF* **1958**, *18*, 74.
(10) Ruiz-Lopez, M. F.; Loos, M.; Goulon, J.; Benfatto, M.; Natoli, C. R. *Chem. Phys.* **1988**, *121*, 419.
(11) Ishii, I.; Hitchcock, A. P. *J. Chem. Phys.* **1987**, *87*, 830.
(12) Rühl, E.; Hitchcock, A. P. *J. Am. Chem. Soc.*, **1989**, *111*, 2614.
(13) Cooper, G.; Sze, K. H.; Brion, C. E. *J. Am. Chem. Soc.*, in press.
(14) Cooper, G.; Sze, K. H.; Brion, C. E. Unpublished work.
(15) Johnson, A. L. Ph.D. Thesis, Berkeley, 1986, LBL-20964.
(16) Hitchcock, A. P.; Beaulieu, S.; Steel, T.; Stöhr, J.; Sette, F. *J. Chem. Phys.* **1984**, *80*, 3927.
(17) McLaren, R.; Clark, S. A. C.; Ishii, I.; Hitchcock, A. P. *Phys. Rev. A.* **1987**, *36*, 1683.
(18) Haaland, A. *Acc. Chem. Res.* **1979**, *12*, 415.

Table I. Energies (E, eV), Oscillator Strengths (f), Term Values (TV, eV), and Proposed Assignments for Features in the C 1s Spectra of Ferrocene, Cobaltocene, and Nickelocene

$Fe(Cp)_2$			$Co(Cp)_2$			$Ni(Cp)_2$			assignment final orbital
E	f	TV[a]	E	f	TV	E	f	TV	
285.72	0.149	4.3	284.81	0.077	5.2	284.38	0.056	5.4	$4e_{1g}$ (M 3d)
287.19[b]	0.280	2.8	286.82[b]	0.291	3.2	286.33[b]	0.323	3.5	$3e_{2u}$(Cp π^*)
289.1		0.9	289.4		0.6	288.3		1.5	Ryd
						288.9		0.9	Ryd
290.0			290.0			289.8			IP (C 1s)[c]
292.0		-2.0	291.9		-1.9	291.3		-1.5	σ^*(C-C)
293.7		-3.7				292.6		-2.8	double excitation
297.7		-7.7	297.7		-7.7	297.5		-7.7	σ^*(C-C)
301 (sh)		-11	302 (sh)		-12	301 (sh)		-11	shake-up ?

[a] TV = IP - E, where IP is the energy of the main XPS line. [b] Calibration relative to CO_2 (1s $\rightarrow \pi^*$, 290.74 eV[41]): Fe, ΔE = -3.55 eV; Co, ΔE = -3.92 eV; Ni, ΔE = -4.41 (3) eV. [c] From XPS.[23]

Table II. Orbital Energies (ϵ, eV) and $2p_z$ Coefficients for Ground State and "C 1s-Excited" Metallocenes from Extended Hückel Theory[a]

orbital			$Fe(Cp)_2$		$Co(Cp)_2$		$Ni(Cp)_2$	
D_{5d}	D_{5h}	char.	$-\epsilon$	$c(C2p_z)^b$	$-\epsilon$	$c(C2p_z)^b$	$-\epsilon$	$c(C2p_z)^b$
			A. Ground State					
$4e_{2g}$	e_2'	π^*	5.77	0	6.41	0	6.38	0
			5.77	0.55	6.41	0.55	6.38	0.55
$3e_{2u}$	e_2''	π^*	6.49	0	6.55	0	6.60	0
			6.49	0.56	6.55	0.56	6.60	0.56
$4e_{1g}$	e_1''	$d_{xz,yz}$	7.76	0	9.67	0	9.85	0
			7.76	0.34	9.67	0.33	9.85	0.36
			B. "C 1s Excited State(s)" $[(NHC_4H_4)M(C_5H_5)]^+$ Equivalent Core Species					
$4e_{2g}$	e_2'	π^*	5.77	0	6.41	0	6.38	0
			6.04	0.14	6.47	0.03	6.43	0.05
$3e_{2u}$	e_2''	π^*	6.49	0	6.55	0	6.60	0
			7.31	0.31	7.86	0.55[c]	7.83	0.55[c]
$4e_{1g}$	e_1''	$d_{xz,yz}$	7.84	0	9.69	0	9.87	0
			8.50	0.61	10.01	0.38[c]	10.26	0.40[c]

[a] The extended Hückel parameters were those reported in ref 19, while the geometries were those of the gas-phase molecule as determined by electron diffraction.[18] Although the D_{5h} symmetry labels are those which are correct for the eclipsed equilibrium geometry, the D_{5d} labels are used in order to conform to common usage. [b] This is the $2p_z$ coefficient at the atom which is converted to N in the Z+1 calculation. Note that, for symmetry reasons, this coefficient is zero in one partner of each e-symmetry orbital. [c] Note that the effect on the intensity of the C 1s $\rightarrow 4e_{1g}$ intensity of the partial occupancy of the $4e_{1g}$ orbital in $Co(Cp)_2$ and $Ni(Cp)_2$ has been taken into account in Figure 3 by a proportional reduction of these orbital coefficients.

of Albright et al.[19] The present EHT results give the accepted orderings of the outermost orbitals in the ground-state electronic structure of the Fe, Co, and Ni metallocenes.

In addition to the ground-state electronic structure, an EHT calculation of the Z+1, equivalent core analogy species, $[(C_4H_4NH)M(Cp)]^+$ was carried out. The eigenfunctions and eigenvalues of this equivalent core ionic species provide a better approximation to the C1s core excited states than the virtual orbitals of the neutral ground state.[21,22] In this approach, the virtual orbital eigenvalues are compared to the experimental term values (TV = IP(C 1s) - E) (see Table I) of the C 1s states, while the $c^2(N2p_z)$ values, i.e., the square of the $2p_z$ atomic orbital coefficient on the core excited atom (the N atom in $[(C_4H_4NH)M(Cp)]^+$, are considered to be estimates of the relative transition intensity. There are C 1s orbitals of appropriate symmetry to provide electric-dipole allowed transitions to virtual orbitals of all symmetries. Table II presents the EHT results for both the ground and C 1s excited states.

3.2. C 1s Spectra: Features below 290 eV. The C1s oscillator strength spectra of $Fe(Cp)_2$, $Co(Cp)_2$, and $Ni(Cp)_2$ [Cp = C_5H_5] are shown in Figure 2. The C 1s ionization thresholds (IPs), taken from XPS,[23] are indicated by the hatched vertical lines in Figure 2. The energies, term values, and proposed assignments are presented in Table I. The oscillator strengths of the first two features in each spectrum were derived from least-squares fits to gaussian line shapes. These results are also listed in Table I.

The metallocene spectra are characterized by two strong resonances in the pre-edge region and two broad features above the C 1s IP. As has been found in previous studies of C 1s excitation in unsaturated organometallics such as the metal carbonyls,[12-14] the C 1s spectra of the metallocenes are dominated by excitations to π^* and σ^* orbitals associated with the cyclopentadienyl ligand. The 1s$\rightarrow\sigma^*$ spectral features (292 and 298 eV) are discussed in greater detail in the following section. In addition to the four strong features, there are weak shoulders in the region around the C 1s IP. These are likely associated with C 1s $\rightarrow$ Rydberg excitations for the features below the IP and double excitations for those above the IP.

Although the positions of the continuum σ^* features are relatively constant through the series, the pre-edge, π^*-like features ($\approx$284, $\approx$287 eV) display appreciable, systematic shifts in their energies and intensities with the complexed transition metal (Table I). This is in distinct contrast to the core excitation spectra of metal carbonyls[12-14] where the energies of the 1s $\rightarrow \pi^*$ transitions are essentially independent of the identity of the metal atom and where there are only relatively minor variations of the oscillator strength per carbonyl with metal type.[12] Although a direct comparison with the cyclopentadienyl anion or radical is not possible since their C1s spectra have not yet been reported [Recently we have recorded the C 1s spectrum of cyclopentadiene as well as that of the Diels-Alder dimer.[24] The C 1s spectrum of the dimer exhibits one strong C 1s $\rightarrow \pi^*$ transition at 284.7 eV, as expected from comparison to the C 1s spectra of other species with isolated double bonds. The spectrum of the monomer

(19) Albright, T. A.; Hofmann, P.; Hoffmann, R. *J. Am. Chem. Soc.* **1977**, *99*, 7546.
(20) Halet, J. F.; Saillard, J. Y.; Lissillour, R.; McGlinchey, M. J.; Jaouen, G. *Inorg. Chem.* **1985**, *24*, 218.
(21) Schwarz, W. H. E. *Angew. Chem., Int. Ed. Engl.* **1974**, *13*, 454.
(22) Schwarz, W. H. E.; Chang, T. C.; Seeger, U.; Huang, K. H. *Chem. Phys.* **1987**, *117*, 73.
(23) Bakke, A. A.; Jolly, W. L.; Schaf, T. F. *J. Electron Spectrosc.* **1977**, *11*, 339. Towan, D. O.; Park, J.; Barber, M.; Swift, P. *Chem. Commun.* **1971**, 1444.

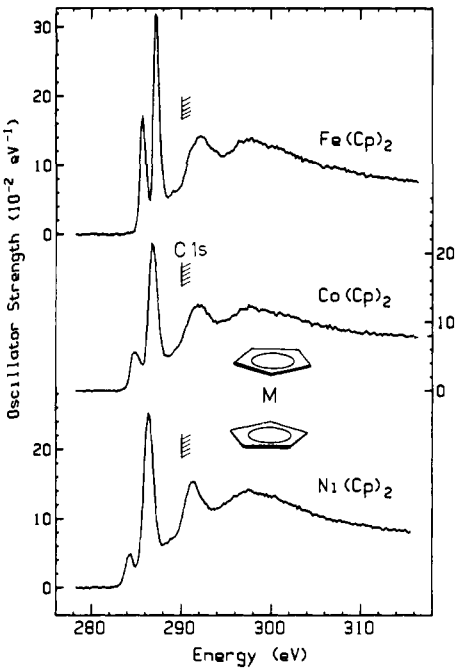

Figure 2. Oscillator strengths for C 1s excitation of ferrocene cobaltocene, and nickelocene derived from electron energy loss spectra recorded with 2.5 keV final electron energy, 2° scattering angle, and 0.7 eV FWHM resolution. After background subtraction to isolate only the 1s signal, the spectra were corrected for a kinematic term and normalized at IP + 25 eV to scaled, calculated atomic oscillator strengths, according to a procedure previously documented.[17] The hatched lines indicate the energies of the main line C1s IPs as determined by XPS.[23]

(C_5H_6) has its principle π^* feature at 285.1 eV, and it also contains a moderately intense second C 1s → π^* peak at 287.4 eV. The C 1s → π^* energies and the 2.4-eV splitting of the two π^* levels are similar to that observed in *trans*-1,3-butadiene.[16,17]] the low-energy π^*-region of the C1s spectrum of cyclopentadienyl should be dominated by a single peak since there is only one empty π^* orbital of e_2'' symmetry in the minimal basis MO scheme of the anion, $C_5H_5^-$ (Cp^-). This transition might be expected to occur around 285 ± 1 eV, based on the C 1s spectra of other aromatic and conjugated hydrocarbons (e.g., the C 1s → π^* transition occurs at 284.6 eV in butadiene[16,17] and 285.3 eV in benzene[25]). However, the shielding effect of the negative charge in Cp^- might raise the C 1s → π^* energy somewhat relative to its energy in the neutral, six-electron aromatics. It is clear that there is a strong qualitative difference between the single π^* feature expected in free Cp^- and the two "π^*-like" features seen in the metallocene C 1s spectra.

The shifts in the absolute energies and term values of the first two transitions through the metallocene series are considerably greater than the shifts in the XPS IPs, indicating relatively large effects of the metal on the energies of the virtual orbitals involved. This is consistent with the electron transmission (ET) spectra of the metallocenes[3,4] where the anion state energies vary considerably. Thus the energy shifts in the first peak in the C 1s spectrum primarily reflect changes in the energies of the virtual orbitals rather than the C 1s orbitals of the metallocenes.

Two interpretations were considered initially for the assignment of these pre-edge features in the metallocene C 1s spectra. One possibility was that the two features are transitions to the two ($3e_{2u}$ and $4e_{2g}$) ring-π^* orbitals. This alternative would be consistent with the dominance of intramolecular transitions in the NEXAFS of molecules chemisorbed on metal surfaces.[25,26] The other possibility was that the first feature is a C 1s → $4e_{1g}(d_{xz},d_{yz})$ transition, while the second consists of unresolved transitions to the two ring-π^* orbitals. We have used the extended Hückel theory (EHT) calculations in order to help choose between these alternatives. The intent of these semiempirical calculations is to search for trends rather than provide highly accurate numerical results. Table II presents the EHT results for both the ground state and C 1s excited states.

According to the magnitude of the carbon 2p coefficients in the ground-state EHT results (Table IIA) there should be three low-lying C 1s excitations, although the C 1s → $4e_{1g}(d_{xz},d_{yz})$ transition would be considerably weaker than the C 1s → π^*(ring), and the two C 1s → π^*(ring) transitions would not be resolved with our spectrometer since the $3e_{2u}$ and $4e_{2g}$ orbitals are very close in energy. The ground-state EHT calculations for the Fe, Co, and Ni species indicate separations of less than 0.8 eV and a large ring-π^* character to both orbitals ($c^2(C2p_z)$ = 0.3) (see Table II), while an Xα calculation indicates 0.16 eV separation in the $Ni(Cp)_2$ ground state.[3] In the absence of strong interaction with occupied $e_{2g}(d)$ orbitals, the $3e_{2u}$ and $4e_{2g}$ ring-π^* orbitals are expected to be very close in energy since they correspond to positive and negative combinations of the e_2'' orbital of each Cp ring which are rather distant from each other (the ring-to-ring separation is >3.3 Å). The EHT calculations indicate that the ring-π^* virtual orbitals are strongly modified by the C 1s core hole. In the core-equivalent species the $3e_{2u}$ orbital is split by ≈1.5 eV, but the orbital shape is not greatly changed while the $4e_{2g}$ orbital is "repelled" from the core excited atom (the $N2p_z$ coefficient becomes very small) and the splitting associated with the symmetry reduction is much smaller than that in the $3e_{2u}$ orbital. Thus the EHT results for the "C 1s excited states" predict only two rather than three pre-edge transitions, which is consistent with the experimental results.

The large $N2p_z$ coefficients for the $4e_{1g}$ and $3e_{2u}$ orbitals in the EHT calculation of the C1s excited states of the Fe, Co, and Ni species strongly supports assignment of the lower energy feature to C 1s → $4e_{1g}(d_{xz},d_{yz})$ and the higher energy peak to C 1s → $3e_{2u}(\pi^*)$ transitions in these three species. The increase in the $4e_{1g}$ occupancy with increased d-count of the metal atom provides a simple explanation of the decrease in the intensity of the first peak. In the ground state the $4e_{1g}$ orbital is composed mainly of metal $3d_{xz}$ and $3d_{yz}$ orbitals ($c^2(C2p_z)$ = 0.11, according to the EHT results—Table II), and thus one would not expect strong C 1s → $4e_{1g}$ transitions on account of the poor spatial overlap. This is also indicated by an Xα calculation of nickelocene which indicates 57% transition metal, 27% p_π, 12% inner sphere, and 4% outer sphere character[3] for the $4e_{1g}$ orbital—i.e., this orbital is very heavily concentrated on the metal. Any ring C2p character to the $4e_{1g}$ orbital can be attributed to mixing with the occupied π orbital of e_1'' symmetry in free Cp^-. According to the EHT results for the equivalent core species (Table IIB), the C2pπ character of the $4e_{1g}$ orbital is greatly enhanced when there is a carbon 1s hole, presumably because the core hole potential lowers the $4e_{1g}(d_{xz},d_{yz})$ orbital energy and increases the π^* character through enhanced mixing with the $3e_{1g}$ (π) orbital.

The spectra show that the C 1s → $4e_{1g}$ intensity is considerably reduced in $Co(Cp)_2$ and $Ni(Cp)_2$ relative to $Fe(Cp)_2$. At first glance this experimental result seems qualitatively different than the EHT result where the $N2p_z$ coefficient in the $4e_{1g}$ orbital is similar in all three molecules (0.61, 0.38, 0.40). However the $4e_{1g}$ orbital is partially occupied—by one electron in $Co(Cp)_2$ and by two electrons in $Ni(Cp)_2$. This will reduce the spectral transition intensity since electron promotions into occupied orbitals are not allowed by the Pauli exclusion principle. The observed change in the intensity of the C 1s → $4e_{1g}$ transition is approximately inversely proportional to the occupancy of the $4e_{1g}$ orbital in these species. Thus we are suggesting that the $4e_{1g}$ orbital is similar throughout the series and that, to first order, the reduced intensity can be related to the changes in ground-state occupancy with metal d-count. In a sense this can be considered to be an extension of the situation in the transition-metal carbonyls where the reduced C 1s → π^*(CO) oscillator strength in the higher d-count species

(24) Hitchcock, A. P.; Wen, A. T.; Rühl, E., manuscript in preparation.
(25) Horsley, J. A.; Stöhr, J.; Hitchcock, A. P.; Newbury, D. C.; Johnson, A. L.; Sette, F. *J. Chem. Phys.* **1985**, *83*, 6099.
(26) Stöhr, J. In *X-ray Absorption: Principles, Applications, Techniques of EXAFS, SEXAFS and* XANES; Konigsberger, D.; Prins, R. L., Eds.; Wiley: New York, 1987. Stöhr, J.; Outka, D. *J. Vac. Sci. Tech. A.* **1987**, *5*, 919.

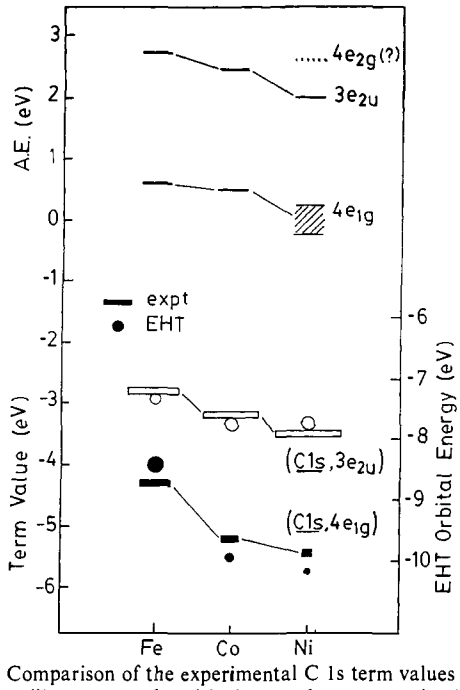

Figure 3. Comparison of the experimental C 1s term values (TV = IP − E) and oscillator strengths with the attachment energies (AE) from electron transmission spectroscopy[3,4] and the orbital energies and squares of N2p_z coefficients from an extended Hückel theory (EHT) calculation of $CpM(C_4H_4NH)^+$. The $4e_{1g}$ orbital coefficients for the Co and Ni species have been reduced from their calculated values in order to account for their partial occupancy. The EHT orbital energy scale has been chosen to give best agreement with the experimental energies. The areas of the circles are proportional to the square of the $2p_z$ coefficient, while the areas of the rectangles are proportional to the experimental oscillator strengths.

has been attributed to increased metal→carbonyl backbonding.[12] However, in the latter case, changes in the C 1s → π^* intensities are related to varying extents of orbital mixing, whereas the dominant effect in the group 8b metallocenes appears to be partial occupancy of the $4e_{1g}$(d) orbital.

The second peak around 287 eV in the Fe, Co, and Ni metallocene C1s spectra is assigned to C 1s → $3e_{2u}(\pi^*)$ transitions with minor contributions from C 1s → $4e_{2g}(\pi^*)$ transitions. This assignment is supported by the EHT results which predict that the C 1s → $4e_{2g}(\pi^*)$ transition will be 5–90 times less intense than the C 1s → $3e_{2u}(\pi^*)$ transition. Experimentally, the ≈287-eV peak increases in intensity with increasing d-count, although much less dramatically than the ≈284-eV peak. The EHT coefficients predict an increase by a factor greater than two in the intensity of the C 1s → $3e_{2u}$ transition between ferrocene and (cobaltocene, nickelocene). No such increase is observed experimentally.

Overall, although there are quantitative differences, particularly in relative intensities, the EHT calculations qualitatively reproduce the main trends in the experimental results. Figure 3 presents a graphical comparison of the experimental term values and oscillator strengths with the EHT orbital energies and N2p_z coefficients for the equivalent core analogy species. The attachment energies (AE) from ETS[3,4] are also plotted. The main quantitative discrepancy between the EHT orbital energies and experimental term values is an average difference of 4.6 eV. Some of the differences between experiment and calculation may be associated with the gross simplification of the use of virtual orbital energies rather than differences of energies of properly constructed electronic states. This could be particularly important for the open shell species where each electron configuration will have several associated electronic states.

The only other core excitation studies of metallocenes of which we are aware are those of the metal K-shell absorption spectra of ferrocene[9,10] and nickelocene.[10] In that work the lowest energy features were identified as very weak transitions to the $4e_{1g}$ orbital; however, the experimental spectra are dominated by M 1s → a_{2u} and M 1s → e_{1u} continuum resonances which have a dominant metal 4p character. Thus the metal K-shell spectra provide a complementary picture since the orbitals accessed and their spatial distribution greatly differ from the orbitals probed in the C 1s spectra.

Our core excitation results are in good agreement with the electronic transmission spectra (ETS) of the metallocenes. Both techniques probe the unoccupied orbitals of the ground state, but the ETS gives a total-molecule picture that is unaffected by the core hole stabilization. The two features observed in the ETS of ferrocene[3,4] have been attributed to population of the $4e_{1g}(d_{xz},d_{yz})$ and $3e_{2u}$ and $4e_{2g}(\pi^*)$ orbitals. Probably both anion states associated with population of the two ring-π^* orbitals are populated, but they are not resolved since, as noted earlier, these two orbitals are the symmetric and antisymmetric combinations of the $e_2''(\pi^*)$ orbital of each Cp ring, and thus the energy separation is small. Interestingly the higher energy negative ion resonance in the ETS of $Ni(Cp)_2$ is clearly split, with the two components at 2.05 and 2.60 eV. In Figure 3 we have suggested this 0.55-eV splitting may correspond to that between the $3e_{2u}$ and $4e_{2g}(\pi^*)$ orbitals. One might expect this splitting to be smallest, and thus unresolved in $Ni(Cp)_2$ since the ring separation is largest in this species. This is the prediction of our EHT calculations; however, other calculations have suggested that the $3e_{2u}$–$4e_{2g}(\pi^*)$ separation is 0.4 eV larger in $Ni(Cp)_2$ than in $Fe(Cp)_2$.[4] The energy spacings of the first two ISEELS bands of the Fe–Ni species are comparable to the ca. 2-eV separation of the first two anion states observed by ETS[3,4] (see Figure 3). The decrease in energy of the $4e_{1g}$ orbital with increasing metal atomic number suggested by the ISEELS term values is also seen in the anion state energies. Overall there is an average core hole stabilization energy (AE − TV) of 5.5 ± 0.2 eV for the $4e_{1g}$ and $3e_{2u}$ orbitals. This is somewhat smaller than the values of 6–8 eV reported in organo-halide compounds,[27] indicating that core hole stabilization varies among different classes of compounds. The $4e_{1g}$ orbital of $Fe(Cp)_2$ has an apparently anomalously low stabilization energy of 4.9 eV.

With regard to the absolute intensities of the C 1s → $\pi^*(3e_{2u})$ transitions in these species, one might expect their oscillator strengths to be comparable to those of C 1s → π^* transitions in other conjugated or aromatic π-bonded species such as butadiene and benzene. The average f-value for the C 1s → π^* transition in these three metallocenes is 0.29/4 = 0.075 per formal double bond. This is quite similar to the oscillator strength per double bond of the C 1s → π^* transition in butadiene (0.14/2 = 0.070[17]) and that in benzene (0.244/3 = 0.081). As has been concluded previously,[17,28] oscillator strengths for localized core excitations in molecules with similar local structures are found to be quite similar.

3.3. 1s → σ^* Continuum Resonances. The cyclopentadienyl rings have 5-fold symmetry and thus have a single C–C bond length. According to a simple model of the relationship between molecular structure and 1s → σ^* transitions[16,29] there should be only a single σ^*(C–C) resonance at about 296 eV. However two continuum peaks are observed in each spectrum around 292 and 298 eV. This pattern is very similar to that found in the C 1s spectra of free and chemisorbed benzene, pyridine,[25] and other six-electron aromatics[30,31] where two continuum resonances are also observed. On the basis of analogy with benzene we interpret these features as one-electron transitions to σ^* shape resonances[25,32] with the average energy reflecting the molecular bond length. The NEXAFS of a monolayer of cyclopentadienyl adsorbed on Pt(111)[15] (Figure 4) is consistent with this interpretation. Two

(27) Benitez, A.; Moore, J. H.; Tossell, J. A. *J. Chem. Phys.* **1988**, *88*, 6691.
(28) Robin, M. B.; Ishii, I.; McLaren, R.; Hitchcock, A. P. *J. Electron Spectrosc.* **1988**, *47*, 53.
(29) Sette, F.; Stöhr, J.; Hitchcock, A. P. *J. Chem. Phys.* **1984**, *81*, 906.
(30) Doering, J. P.; Gedanken, A.; Hitchcock, A. P.; Fischer, P.; Moore, J.; Olthoff, J. K.; Tossell, J.; Raghavachari, K.; Robin, M. B. *J. Am. Chem. Soc.* **1986**, *108*, 3602.
(31) Newbury, D. C.; Ishii, I.; Hitchcock, A. P. *Can. J. Chem.* **1986**, *64*, 1145.
(32) Hitchcock, A. P.; Stöhr, J. *J. Chem. Phys.* **1987**, *87*, 3253.

continuum features are observed at 292 and 298 eV in the Cp/Pt(111) spectrum, and each one has the polarization dependence of an inplane C 1s → σ* transition, assuming that the plane of the ring is parallel to the Pt surface. However, there is evidence from NEXAFS of benzene on Cu(110),[33] partial cross sections,[34] and calculations[22] that suggests ($\underline{1s,\pi,\pi^{*2}}$) double excitations also contribute to the lower energy continuum feature in benzene. Perhaps a similar situation exists in the C1s spectrum of the metallocenes. If one considers only the higher energy feature to correspond to bond length sensitive 1s → σ*(C–C) transition, then the bond length correlation for $Z = 12$[29] predicts a bond length of 1.43 Å, in excellent agreement with the known structures (R_{cc} = 1.43 Å in nickelocene and 1.44 Å in ferrocene[18]).

3.4. Comparison with NEXAFS Studies of π-Bonded Aromatics. In essentially all of the NEXAFS of chemisorbates studied to date[26] the core excitation spectra have been found to be dominated by transitions within the chemisorbed molecule. The major effect of the surface metal atoms on the spectra seems to be a line broadening which has been attributed to lifetime reductions associated with hybridization of the metal and molecule electronic structure.[35] Given that the surface bond in many cases has a strength comparable to many covalent bonds, it seems surprising that there is relatively little evidence for surface-induced modifications of the adsorbate virtual electronic structure. The addition of the C 1s → $4e_{1g}$ transition and the relatively large energy shifts in the spectral features with identity of the metal atom indicates that the virtual orbitals accessed by C1s excitation of the metallocenes differ dramatically from those of free Cp, i.e., the virtual orbitals of Cp attached to a metal are no longer just those intrinsic to the Cp ligand but rather have a large metal admixture. Although this result is not surprising from MO theory, it does contradict a frequent, implicit assumption used in the interpretation of NEXAFS of chemisorbates. Thus the present results provide an important caution to NEXAFS interpretations which ignore modifications to the virtual orbital structure of chemisorbates associated with the metal bonding.

The observation of major changes in the C 1s spectra of the metallocenes relative to that expected for free Cp^- suggests that the C 1s NEXAFS of adsorbed cyclopentadienyl or similar π-bonded aromatics may be a good place to look in greater detail for evidence of changes of virtual electronic states induced by surface bonding. A study of the temperature dependence of the vibrational spectra of cyclopentene adsorbed on a Pt(111) surface[36] suggested that cyclopentadienyl is the stable end product when this surface is heated. Recently Johnson[15] has reported the NEXAFS of this surface, but a full interpretation of the spectrum was not carried out, in part because of the lack of spectra of gas-phase models and in part because of possible uncertainty in the nature of the surface species. In Figure 4 we plot the surface NEXAFS spectra[15] in comparison with the C 1s spectrum of $Ni(Cp)_2$, which is valence isoelectronic with $Pt(Cp)_2$. A linear background has been subtracted from the NEXAFS data to isolate the C1s signal.

The NEXAFS of the monolayer Cp/Pt(111) state produced by room temperature annealing of cyclopentene, consists of a broad, structured π* resonance (peak at 287 eV, shoulder at 285 eV) and two σ* resonances at 291.7 and 297.5 eV. In the original discussion[15] only a single π* resonance is mentioned, but it is clear that there are at least two electronic states in the π* region, just as we find for the metallocenes. Although the first π* peak is considerably more intense than in the metallocenes and all features are broader, the qualitative agreement with the present metallocene spectra adds further support to the conclusion that a cyclopentadienyl species, oriented flat on the Pt(111) surface, is formed

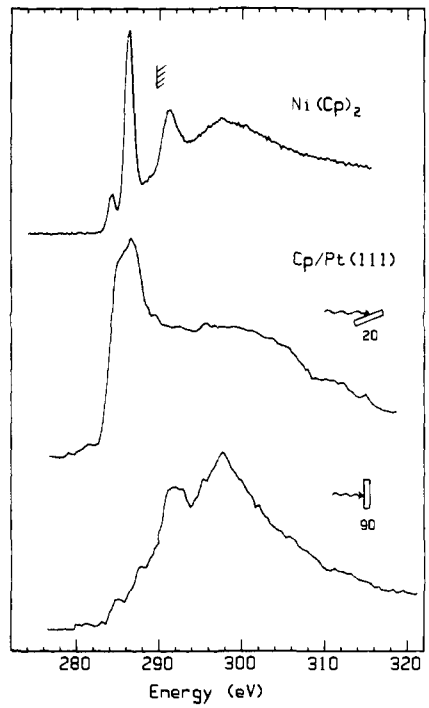

Figure 4. Comparison of the C 1s spectrum of gas-phase $Ni(Cp)_2$ and the NEXAFS spectra of Cp/Pt(111)[15] (the surface state derived from room temperature annealing c-C_5H_8 adsorbed at 90 K onto Pt(111)). Assuming that the ring lies flat on the metal surface, the orientation dependence of the NEXAFS clearly demonstrates π-symmetry for the 285- and 287-eV features and σ-symmetry for the 292- and 298-eV features.

under these conditions. The change from the C 1s spectrum of cyclopentene[15,37] is dramatic and consistent with that expected for conversion in the adsorbed phase to an aromatic electronic structure (i.e., increased π* resonance intensity, along with increased resonance width and a shift to higher energy associated with metal-molecule orbital mixing). Comparison to the C1s spectrum of $Ni(Cp)_2$ reveals that the low-energy shoulder on the π* band is an expected spectral feature. Indeed, it is a distinctive feature associated with the chemisorption bond since free Cp^- would be expected to have only a single C 1s → π* feature. The present results suggest that additional low-lying C 1s → π*-(metal-ring) resonances could be a general feature of π-bonding to metals. This is relevant to studies of other π-bonded adsorbates, such as the NEXAFS of benzene on Pt(111),[25] Ag(111), Cu(100),[33] and Ag(100)[38] and the near-edge energy-loss fine structure (NEELFS) of benzene and pyridine on Cu and Ag(100).[39] The occurrence of strong metal participation in the unoccupied electronic structure of chemisorbed molecules has previously been indicated through Xα calculations in the case of ethylidene on Pt(111).[40]

4. Summary

C1s core excitation spectra of the group 8b 3d-metallocenes have been presented for the first time. The spectra are dramatically different from that expected for the free cyclopentadienyl ligand. They also show a very strong dependence of the near-edge π* features on the nature of the metal atom. These results are in strong contrast to the C 1s spectra of transition metal carbonyls where the spectra are found to be largely independent of the metal atom. A major part of the difference seems to be related to the

(33) Bader, M.; Haase, J.; Frank, K.-H.; Ocal, C.; Puschmann, A. *J. Phys. Coll.* **1986**, *47*, C8-491.
(34) Piancastelli, M. N.; Ferrett, T. A.; Lindle, D. W.; Medhurst, L. J.; Heimann, P. A.; Liu, S. H.; Shirley, D. A. *J. Chem. Phys.* **1988**, *89*, 6096.
(35) Jugnet, Y.; Himpsel, F. J.; Avouris, Ph; Koch, E. E. *Phys. Rev. Lett.* **1984**, *53*, 198.
(36) Avery, N. *Surf. Sci.* **1984**, *137*, L109; **1984**, *146*, 363. Netzer, F. P.; Rosina, G.; Bertel, E.; Saalfeld, H. B. *J. Electron Spectrosc.* **1988**, *46*, 373.
(37) Hitchcock, A. P.; Newbury, D. C.; Ishii, I.; Stöhr, J.; Horsley, J. A.; Redwing, R. D.; Johnson, A. L.; Sette, F. *J. Chem. Phys.* **1986**, *85*, 4849.
(38) Stöhr, J., private communication.
(39) Tyliszczak, T.; Esposto, F.; Hitchcock, A. P. *Phys. Rev. Lett.* **1989**, in press.
(40) Horsley, J. A.; Stöhr, J.; Koestner, R. J. *J. Chem. Phys.* **1985**, *83*, 3146.
(41) Hitchcock, A. P.; Ishii, I. *J. Electron Spectrosc.* **1987**, *42*, 11.

open shell electronic structure of these metallocenes and an appreciable ring π^* character to the empty or partially filled metal 3d orbitals. The core hole polarization in the C 1s excited states has a considerable effect on the spatial distributions of the virtual orbitals according to the EHT calculations.

Acknowledgment. This work was financed by the Natural Science and Engineering Research Council of Canada (NSERC). We thank Drs. J. Stöhr and A. L. Johnson for commentary and permission to use their NEXAFS data, and Dr. M. J. McGlinchey for helpful comments and assistance with the extended Hückel calculations. A.P.H. acknowledges the support of an NSERC university research fellowship.

Registry No. $Fe(C_5H_5)_2$, 102-54-5; $Co(C_5H_5)_2$, 1277-43-6; $Ni(C_5H_5)_2$, 1271-28-9.

Quantitative Study of the Acidity of HCl in a Molten Chloroaluminate System ($AlCl_3$/1-Ethyl-3-methyl-1*H*-imidazolium Chloride) as a Function of HCl Pressure and Melt Composition (51.0–66.4 mol % $AlCl_3$)

G. P. Smith, A. S. Dworkin, R. M. Pagni,[1] and S. P. Zingg*

Contribution from the Chemistry Division, Oak Ridge National Laboratory, Oak Ridge, Tennessee 37831. *Received December 2, 1988*

Abstract: The acidity of HCl in Lewis acid mixtures of $AlCl_3$ and 1-ethyl-3-methyl-1*H*-imidazolium chloride (EMIC) has been determined as a function of HCl pressure (P_{HCl}) and melt composition at ambient temperatures. The equilibrium constant (K'_B) for the protonation of arene bases (B) according to the reaction $HCl + B \rightleftarrows BH^+ + Cl^-$ was determined from the relation $\log K'_B = H' + \log([BH^+]/[B])$ with the protonation ratio measured spectrophotometrically and the acidity function, $H' = \log([Cl^-]/P_{HCl})$, evaluated by using the thermodynamic model of Dymek et al. to calculate $[Cl^-]$. Values of $\log K'_B$ were determined for chrysene, fluorene, 2-methylnaphthalene, and mesitylene over a range of HCl pressures and melt compositions, while estimates for benzene, toluene and naphthalene were obtained at a single pressure and composition (1 atm, 66.4 mol % $AlCl_3$). The correlation between $\log K'_B$ for these arenes in HCl/$AlCl_3$–EMIC and $\log K_B$ for the same arenes in HF/BF_3 suggests that $H' - H_0 \simeq 0.4$, where H_0 is the Hammett acidity function. According to this criterion H_0 for 0.01 atm HCl in 51 mol % $AlCl_3$ has a value of −12.6 (a superacid comparable to 100% H_2SO_4). At 1 atm HCl, a melt saturated with $AlCl_3$ at ambient temperatures (~67 mol % $AlCl_3$) is a much stronger superacid with a value of H_0 on the order of −18.

We recently showed[2] that when HCl is dissolved in a molten mixture of $AlCl_3$ and 1-ethyl-3-methyl-1*H*-imidazolium chloride (EMIC) containing 55.0 mol % $AlCl_3$ at ordinary temperatures and pressures it becomes a Brønsted superacid similar in strength to liquid HF ($H_0 = -15.1$[3]). The acidity of this mixture was determined by spectrophotometrically measuring the protonation of arene bases. 2-Methylnaphthalene proved to be a base of intermediate strength and was used for a quantitative study of the effect of HCl pressure on the Brønsted acidity. The results were consistent with the following simple chemical model. The protonation of an arene base (B) in an acidic $AlCl_3$–EMIC melt, i.e., one containing significantly more than 50 mol % $AlCl_3$, can be represented for thermodynamic purposes by eq 1. The

$$HCl + B \rightleftarrows BH^+ + Cl^- \quad (1)$$

stoichiometric equilibrium constant for this reaction (K'_B) is given by eq 2, where $pK'_B = -\log K'_B$, Π is the protonation ratio

$$pK'_B = -\log \Pi + pCl + \log P_{HCl} \quad (2)$$

($[BH^+]/[B]$), $pCl = -\log [Cl^-]$, and P_{HCl} is the pressure in atm of HCl in equilibrium with the melt. In these experiments pCl was fixed by the Cl^- exchange equilibrium given in eq 3, so that P_{HCl} was the only variable that affected the system acidity.

$$Cl^- + Al_2Cl_7^- \rightleftarrows 2AlCl_4^- \quad (3)$$

Table I. Spectra of Arenium Ions in $AlCl_3$–EMIC (66.4 mol % $AlCl_3$) under ~1 atm HCl at 23 °C

starting arene	λ_{max} (nm) [$10^{-3}\epsilon$ (M^{-1} cm^{-1})]
fluorene	382 [33.3 ± 0.5[a,b]]
chrysene	268 [27.9], 296 [18.2], 340 [21.5], 525 [18.9 ± 0.3[a,b]]
2-methylnaphthalene	270 [3.6 ± 0.1[c]], 400 [17.8 ± 0.4[a,c]]
mesitylene	262 [10.2], 360 [10.7[a]]

[a] Band used to measure α. [b] Average of two independent measurements. [c] Average of three independent measurements.

We have now extended these studies to include melt composition as a variable, from 51.0 to 66.4 mol % $AlCl_3$. (The latter value is close to the solubility limit for $AlCl_3$ at ambient temperatures.[4]) We will show that the protonation of arenes of intermediate basicity responds to these changes in melt composition in the way described by eq 2 when pCl is calculated from previously measured thermodynamic properties of $AlCl_3$–EMIC melts.[5] Then we will examine the protonation of weakly basic arenes, including benzene. With these results we compare HCl/$AlCl_3$–EMIC with other strong Brønsted acids. In making this comparison it is instructive to treat eq 2 in terms of acidity function formalism. We define

(1) Department of Chemistry, University of Tennessee, Knoxville, TN 37996.
(2) Smith, G. P.; Dworkin, A. S.; Pagni, R. M.; Zingg, S. P. *J. Am. Chem. Soc.* **1989**, *111*, 525.
(3) Gillespie, R. J.; Liang, J. *J. Am. Chem. Soc.* **1988**, *110*, 6053.
(4) Fannin, A. A., Jr.; Floreani, D. A.; King, L. A.; Landers, J. S.; Piersma, B. J.; Stech, D. J.; Vaughn, R. L.; Wilkes, J. S.; Williams, J. L. *J. Phys. Chem.* **1984**, *88*, 2614.
(5) (a) Hussey, C. L.; Scheffler, T. B.; Wilkes, J. S.; Fannin, A. A., Jr. *J. Electrochem. Soc.* **1986**, *133*, 1389. (b) Dymek, C. J., Jr.; Hussey, C. L.; Wilkes, J. S.; Øye, H. A. In *Proceedings of the Joint International Symposium on Molten Salts*; Mamantov, G., Blander, M., Hussey, C., Mamantov, C., Saboungi, M.-L., Wilkes, J., Eds.; The Electrochemical Society Softbound Proceedings Series: Princeton, NJ, 1987; p 93.

0002-7863/89/1511-5075$01.50/0